Available online at www.sciencedirect.com
ScienceDirect
Microporous and Mesoporous Materials 103 (2007) 82–93
MICROPOROUS AND MESOPOROUS MATERIALS
www.elsevier.com/locate/micromeso

Interaction of water vapour at 298 K with Al-MCM-41 materials synthesised at room temperature

P.A. Russo [a], M.M.L. Ribeiro Carrott [a,*], A. Padre-Eterno [a], P.J.M. Carrott [a], P.I. Ravikovitch [b], A.V. Neimark [c]

[a] *Centro de Química de Évora and Departamento de Química, Universidade de Évora, Colégio Luís António Verney, 7000-671 Évora, Portugal*
[b] *Center for Modelling and Characterization of Nanoporous Materials, TRI/Princeton, Princeton, NJ 08542-0625, USA*
[c] *Department of Chemical and Biochemical Engineering, Rutgers University, Piscataway, NJ 08854-8058, USA*

Received 27 November 2006; received in revised form 11 January 2007; accepted 13 January 2007
Available online 26 January 2007

Abstract

The interaction of water vapour with Al-MCM-41, prepared by direct synthesis at ambient temperature and pressure, using tetraethoxysilane, aluminium sulfate, hexadecyltrimethylammonium bromide and ammonia, and its effect on the pore structure were studied in order to investigate the stability towards prolonged exposure to water vapour and the influence of the aluminium content. With this purpose two consecutive water adsorption isotherms were determined at 298 K on samples with Si/Al ratio between 15 and 100. The samples were characterised by X-ray diffraction and adsorption of nitrogen at 77 K and toluene at 298 K, prior to and after exposure to water vapour. Pore size distributions were calculated from nitrogen, toluene and water adsorption isotherms using, respectively, the NLDFT method, a recently developed hybrid MC-DBdB method and the DBdB macroscopic approximation. It was found that Al-MCM-41 samples are significantly stable and that the stability improves as the amount of aluminium increases. Upon prolonged exposure to water vapour, there is a small decrease in pore size (3–5%), pore volume (8–16%) and total surface area (3–7%). The structural changes are essentially a consequence of the surface hydroxylation that occurred and not a result of a partial collapse of the pore structure. Although the presence of some extraframework Al can contribute to the improvement of the stability by protecting the surface, it was concluded that tetracoordinated Al plays an important role. The stabilizing effect of the Al incorporated in the walls can result from a higher degree of condensation on the surface of the pore walls and from the mild acidity generated.
© 2007 Elsevier Inc. All rights reserved.

Keywords: Water adsorption isotherms; Nitrogen and toluene adsorption isotherms; Room temperature synthesised Al-MCM-41; Structural stability; Pore size distributions

1. Introduction

MCM-41, with a porous structure consisting of an hexagonal array of unidirectional cylindrical pores of uniform size, is one of the members of ordered mesoporous materials most studied, whose extraordinary features, disclosed in 1992 [1,2], include high surface areas and pore volumes, tunable pore size and the possibility of incorporation of heteroatoms into the silica structure. This set of characteristics makes them attractive for fundamental studies as well as for applications in the fields of adsorption and catalysis, especially when bulky molecules, that do not fit into the pores of usual adsorbents and catalysts such as zeolites, are involved. In particular, the introduction of aluminium into the MCM-41 structure is of special interest because it generates acidity. Although the acid strength of these materials is not yet at the required levels for processes such as catalytic cracking [3], they can have an interesting performance in other catalytic processes involving large molecules and requiring mild acidity [4–8].

* Corresponding author. Tel.: +351 266745320; fax: +351 266745303.
E-mail address: manrc@uevora.pt (M.M.L. Ribeiro Carrott).

1387-1811/$ - see front matter © 2007 Elsevier Inc. All rights reserved.
doi:10.1016/j.micromeso.2007.01.032

Another limiting aspect for their application in fluidized catalytic cracking is the low hydrothermal stability during the regeneration process to remove the coke [5]. The hydrothermal stability, in boiling water or steam at high temperatures, of aluminium containing MCM-41 has been considered in several publications and, as with silica grades [9], it seems to be dependent on the synthesis conditions [10,11] and, in particular, on the aluminium content. For example, although higher hydrothermal stability has been found for Al-MCM-41 compared with pure silica materials [12–15], with Al grafted MCM-41 appearing to have superior stability to that of directly synthesised materials [16–19], several studies have indicated that hydrothermal stability decreases with the increase of Al content [3,14,18]. It has been demonstrated that improvement of hydrothermal stability of aluminosilicate samples can be achieved through control of the synthesis conditions to lead to thicker and more highly condensed pore walls [20,21].

Other processes, in catalysis and also in adsorption, do not require high hydrothermal stability, but the presence of water or water vapour at room temperature can be a limiting factor. It has been reported that structural degradation of pure silica MCM-41 materials can occur even at 298 K if the material is exposed to water vapour for prolonged periods [22–24], the extent depending on synthesis conditions [24,25]. Improvement of stability can be achieved by modification of the surface with organosilanes [15,22,24,26–30], by pyrolytic carbon deposition [31] or by post-synthesis silicification, using tetraethoxysilane in hexane [32]. With Al-MCM-41 different behaviour, varying from good stability [15,33,34] to irreversible collapse upon hydration [23], has also been reported for different materials. Recently, we have shown that Al-MCM-41 with Si/Al = 30 prepared by a room temperature procedure previously developed by others [35] using aluminium isopropoxide as metal source, was considerably more stable to prolonged exposure to water vapour [36] than pure silica grades, prepared at room temperature or hydrothermally [24], and presented slightly higher stability than an Al-MCM-41 sample prepared using an hydrothermal procedure [37]. Moreover, samples prepared by this method catalysed the reaction of the double bond position of 1-butene to 2-butene and exhibited similar to or better conversions than those prepared by some hydrothermal routes [37].

The promising results just referred to suggest that it would be worthwhile exploring in more detail the interaction of water vapour at 298 K with samples prepared at room temperature in order to evaluate if this stability behaviour would extend to other metal contents and samples prepared with other metal sources, namely aluminium sulfate, which has been shown to be a good alternative to aluminium isopropoxide [37]. Therefore, in this paper, we present a detailed study of the effects of prolonged exposure to water vapour at 298 K, based on the determination of consecutive water adsorption–desorption isotherms and on the results of XRD and adsorption isotherm measurements of nitrogen at 77 K and toluene at 298 K, determined before and after prolonged exposure to water vapour. MCM-41 samples with nominal Si/Al molar ratios of 15, 30, 50 and 100 were studied in order to evaluate the effect of the aluminium content.

2. Materials and methods

2.1. Experimental

The Al-MCM-41 materials have been prepared by direct synthesis at ambient temperature and pressure, using tetraethoxysilane, aluminium sulfate, hexadecyltrimethylammonium bromide and ammonia. The synthesis procedure was previously described [37] and was based on that developed by other authors [35], but with some variations to adapt to the different metal source. Samples with Si/Al = 30 and 15 were obtained from the same uncalcined batch of Al41-S(30)a and Al41-S(15)a of the previous work [37].

The X-ray diffraction (XRD) measurements were carried out on a Bruker AXS-D8 Advance powder diffractometer, using Cu Kα radiation (40 kV, 30 mA), with a step size of 0.01° (2θ) and 5 s per step.

Nitrogen adsorption isotherms at 77 K were determined on a CE Instruments Sorptomatic 1990 using helium (Linde) and nitrogen (Air Liquide) of 99.999% purity. Prior to the adsorption measurements all samples were outgassed at 453 K for 8 h.

The toluene and water vapour adsorption isotherms at 298 K were determined gravimetrically in an apparatus equipped with a CI Electronics MK2 vacuum microbalance and an Edwards Barocel 622 (0–100 mbar) capacitance manometer. The temperature of the circulating liquid jacket around the balance tubes was controlled within ±0.1 K using a Grant LTD thermostat and a Masterflex peristaltic pump. Blank measurements indicated that buoyancy corrections were negligible. The sensitivity and reproducibility of weight readings allowed a reproducibility of the amounts adsorbed better than 1 or 4 μmol g^{-1} for toluene or water, respectively. Toluene and water were used after being purified by double distillation and then outgassed in the vacuum rig by repeated freeze-thaw cycles. Initially and between runs all samples were outgassed at 453 K for 8 h. The saturation pressure and density of each adsorptive at the working temperature were calculated from the data and equations given in the literature [38]. The water measurements took on average 3–4 weeks for each sample due to the long equilibration times.

2.2. Calculation of pore size distributions

Pore size distributions were calculated from nitrogen adsorption isotherms using the NLDFT method [39] and from toluene adsorption isotherms using a recently developed hybrid MC-DBdB method [40].

Pore size distributions were also calculated from water desorption isotherms using the Derjaguin–Broekhoff–de

Boer macroscopic approximation [41,42] (see also [43] for detailed description of the theory). The theory requires an equation for the adsorption film thickness on a non-porous substrate (disjoining pressure isotherm). Water adsorption is very sensitive to the chemistry of the surface, i.e., the number of hydroxyl groups. Usually, the first adsorption isotherm, results in significantly lower adsorption per unit of surface area compared to subsequent adsorption isotherms on the rehydroxylated surface [44]. While the amount adsorbed per unit area may vary, the shape of water isotherms after the completion of the monolayer on different materials is quite similar, and can be approximated by a common t-curve [45,46]. Therefore, the most important parameter from the point of view of estimating the pore size distributions is the absolute amount adsorbed per unit area. We used a water isotherm on a non-porous alumina surface as reported by Naono and Hakuman [47]. The BET C-constant for this isotherm is ca. 26, and the monolayer adsorption corresponds to $P/P_o = 0.18$. The amount adsorbed in the monolayer is ca. 13 μmol/m^2 or 7.8 H_2O/nm^2. When expressed as the number of adsorbed layers, the isotherm is quite similar to the isotherms reported by Hagymassy et al. [45] and Raoof et al. [46]. We approximated this isotherm using the following equation for the disjoining pressure isotherm (film thickness h):

$$\ln(P/P_0) = -\frac{k}{h^m}$$

with the parameters $K = 9.5$ and $m = 2$, where h is in Angstroms. Other parameters for water adsorption were the surface tension of 72 mN/m, and the molar liquid volume $V_L = 0.018$ m^3/mmol.

3. Results and discussion

3.1. Characterisation of original samples by XRD, nitrogen and toluene adsorption

The powder X-ray diffraction patterns presented in Fig. 1, are typical of MCM-41 materials, showing three to four diffraction peaks which can be indexed to a two-dimensional hexagonal lattice. Although the XRD patterns show that all samples have regular pore structures, those corresponding to samples with Si/Al ratios 100 and 50 are better resolved, being composed of four peaks. In addition, the intensity of all the diffraction peaks slightly decreases as the aluminium content in the material

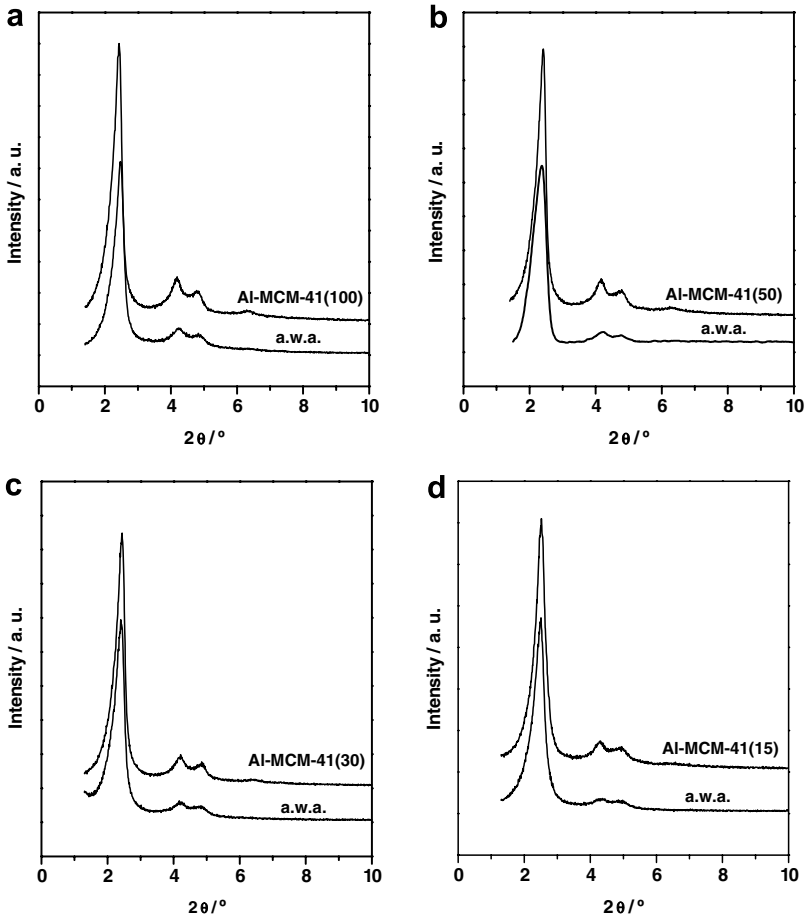

Fig. 1. Powder X-ray diffraction patterns prior to and after water adsorption (a.w.a) of Al-MCM-41 materials with Si/Al of: (a) 100; (b) 50; (c) 30 and (d) 15.

increases, which indicates that the incorporation of Al occurs at the expense of some loss of structural regularity, in a greater extent than titanium using a similar room temperature procedure [36,48].

The nitrogen adsorption isotherms determined on the Al-MCM-41 samples and shown in Fig. 2 are all type IVc [49], completely reversible and exhibiting a steep capillary condensation step, indicating uniformity of the cylindrical pore sizes. The toluene isotherms, as shown in Fig. 3, are similar to those of nitrogen except in the position of the condensation step, which occurs at lower P/P_o, as previously found also on pure silica ordered mesoporous materials [40].

The surface areas and pore volumes presented in Table 1 and 2, respectively, for nitrogen and toluene, were obtained in the usual manner [44,49] from the slopes and intercepts of the α_s plots, respectively, which were constructed using data for the adsorption of the corresponding adsorptive on non-porous partially hydroxylated silica [49]. The first linear region prior to mesopore filling, of each nitrogen α_s plot, could be back-extrapolated through the origin, indicating the absence of primary micropores. Therefore an estimate of mesopore diameter is provided by the values of $D_p(g)$ also presented in Table 1 which were calculated, using the unit cell parameter values, a_o, obtained by XRD, and the nitrogen mesopore volume, on the basis of geometrical considerations for the ideal model of an hexagonal array of non-intersecting cylindrical pores.

From the nitrogen adsorption results in Table 1 it can be seen that all samples have high surface areas and high pore volumes. The low external areas exhibited together with the proximity between the values of V_p and total adsorbed volume at $P/P_o = 0.90$ ($V_{0.9}$) indicates that practically all surface area corresponds to internal surface of mesopores. As the mesopore surface areas obtained by the α_s method are overestimated, as it is well known, the mesopore surface areas were also obtained by the NLDFT method. The results, also presented in Table 1, are about 20% lower than those obtained by α_s method. On the other hand, the mesopores volumes obtained by α_s and NLDFT are in excellent agreement with each other.

For toluene the total surface area values are not presented as the α_s results evidenced an enhancement of the adsorption in the first linear region, as previously noticed also for neopentane on pure silica [50]. There is a good agreement of the external surface areas obtained from nitrogen and toluene α_s plots after pore filling. On the other hand, the toluene pore volumes are in all cases smaller than

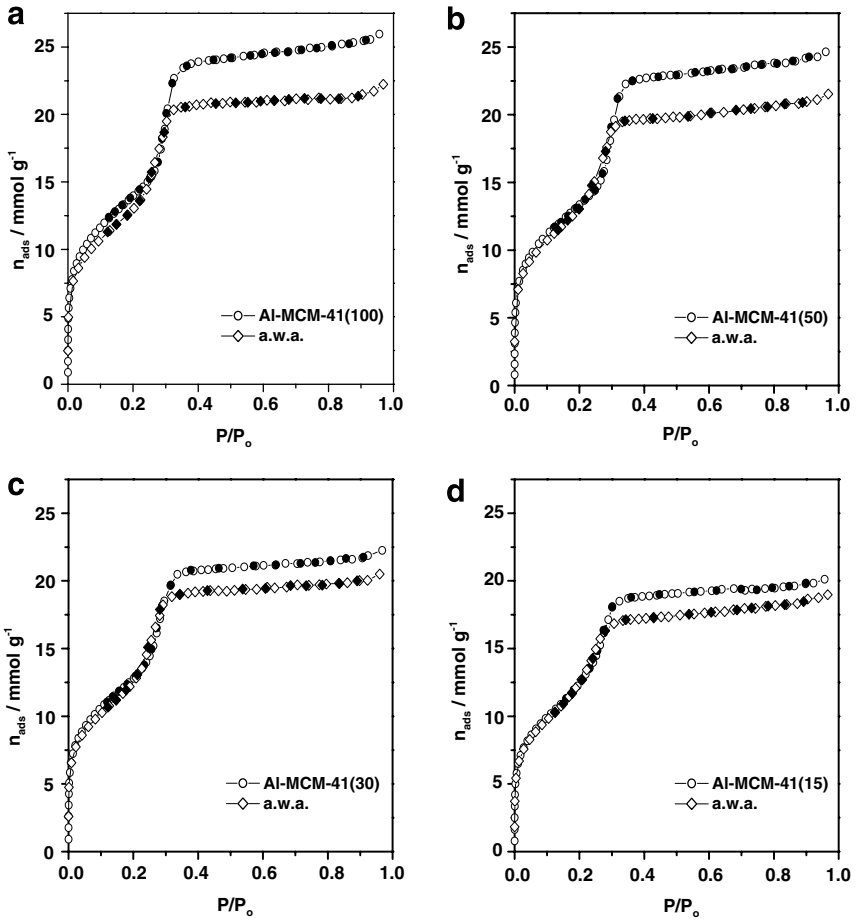

Fig. 2. Nitrogen adsorption isotherms at 77 K determined prior to and after water adsorption (a.w.a) on Al-MCM-41 materials with Si/Al of: (a) 100; (b) 50; (c) 30 and (d) 15 (empty symbols: adsorption, filled symbols: desorption).

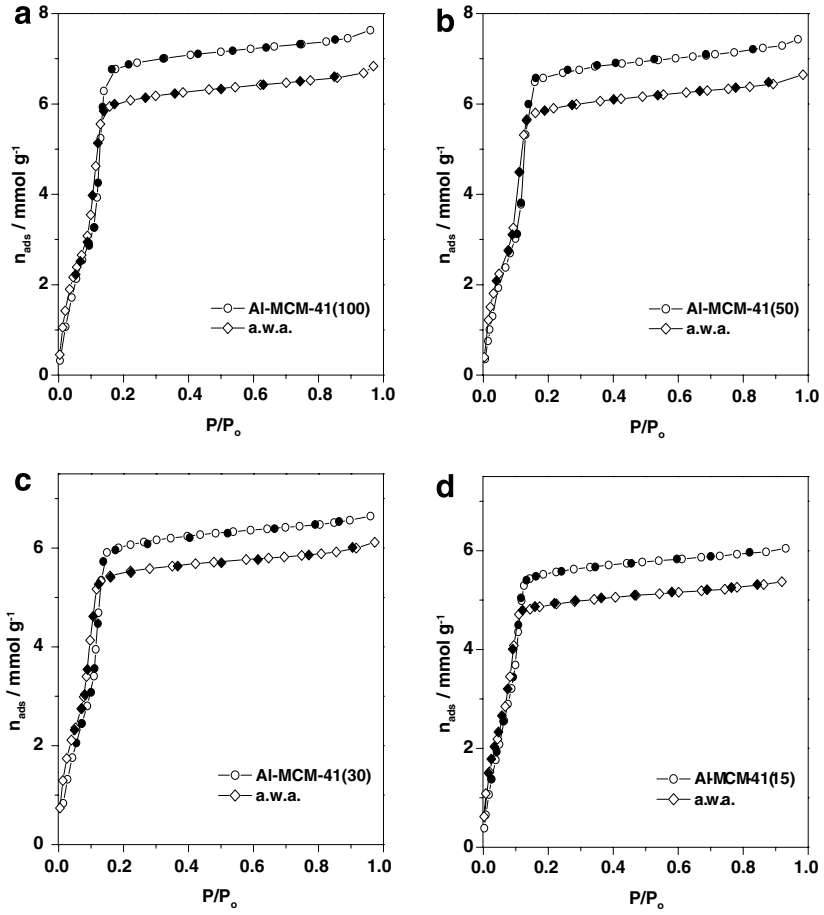

Fig. 3. Toluene adsorption isotherms at 298 K determined prior to and after water adsorption (a.w.a) on Al-MCM-41 materials with Si/Al of: (a) 100; (b) 50; (c) 30 and (d) 15 (empty symbols: adsorption, filled symbols: desorption).

those obtained from the nitrogen isotherms. This difference is not surprising as similar results were previously obtained with other hydrocarbons [50] and also toluene [40] on Si-MCM-41, and can be due mainly to the existence of roughness on the surface of the pore walls which excludes the bulkier organic molecules. In fact, different authors have considered that the pore walls of the MCM-41 materials are not smooth but that instead they exhibit considerable roughness [51–53].

The pore size distributions presented in Fig. 4 were calculated by application of the NLDFT and MC-DBdB methods to the nitrogen and toluene adsorption isotherms, respectively. The pore size distributions indicate good uniformity of the original samples, especially materials with high Si/Al ratio. The widths of the distributions are slightly wider for toluene. We have estimated the pore diameters from the median of the pore size distributions, and the values are presented in Tables 1 and 2. Consistent results (to within 0.15 nm) have been obtained from nitrogen and toluene. In addition, the values are also in good agreement with those of D_p(g).

If a comparison is made between the NLDFT pore sizes and hydraulic pore widths (not shown), calculated using the results from α_s analysis as $d_p(H) = 4V_p/(A_s - A_{ext})$, the values obtained for nitrogen cross sectional area are between 0.134 and 0.14 nm^2. These results are similar to those previously found for pure silicas [50,54] and also for aluminosilicate samples based on comparison from nitrogen and argon BET surface areas [55].

A general overview of the results shows that with increasing aluminium content, the external surface areas remain practically constant, and there is a decrease of the pore volume, total surface area and pore diameter, although not very drastic, as also found in previous studies on other aluminosilicate samples [56].

3.2. Water vapour adsorption

The two consecutive water adsorption–desorption isotherms determined at 298 K on the four Al-MCM-41 with Si/Al ratios 100, 50, 30 and 15, are shown in Fig. 5. A general overview of the results points to some common features with those previously obtained on pure silica grades [24], although there are some important differences which will be discussed and that clearly indicate a higher stability of the aluminium containing samples.

In all cases, both adsorption isotherms present a steep capillary condensation step and exhibit a large hysteresis

Table 1
Pore structural characteristics obtained by analysis of XRD patterns and of nitrogen adsorption isotherms at 77 K, before and after water adsorption (a.w.a.), of Al-MCM-41 samples prepared at ambient temperature and pressure[a]

Sample	a_o (nm)	A_s ($m^2 g^{-1}$)	A_{ext} ($m^2 g^{-1}$)	V_p ($cm^3 g^{-1}$)	$V_{0.9}$ ($cm^3 g^{-1}$)	A_p(DFT) ($m^2 g^{-1}$)	V_p(DFT) ($cm^3 g^{-1}$)	D_p(DFT) (nm)	D_p(g) (nm)	t (nm)
Al-MCM-41(100)	4.28	1082	40	0.83	0.88	880	0.82	3.70	3.61	0.58
a.w.a.	4.17	1004	37	0.70	0.74	800	0.71	3.55	3.41	0.62
Al-MCM-41(50)	4.26	1035	35	0.79	0.84	840	0.78	3.70	3.56	0.56
a.w.a.	4.26	998	37	0.68	0.73	770	0.67	3.50	3.46	0.76
Al-MCM-41(30)	4.21	986	33	0.72	0.75	800	0.71	3.60	3.46	0.61
a.w.a.	4.23	953	35	0.65	0.69	760	0.65	3.50	3.41	0.73
Al-MCM-41(15)	4.11	930	35	0.65	0.68	750	0.64	3.50	3.31	0.61
a.w.a.	4.10	901	36	0.60	0.64	710	0.59	3.35	3.25	0.75

[a] a_o – unit cell parameter; A_s, A_{ext} and V_p – total surface area, external surface area and mesopore volume (in terms of equivalent liquid volume) obtained by the α_s method; $V_{0.9}$ – volume adsorbed at 0.9p° (in terms of equivalent liquid volume); A_p(DFT), V_p(DFT) and D_p(DFT) – mesopore surface area, mesopore volume and mesopore diameter calculated using NLDFT method [39]; $D_p(g)$ – mesopore diameter calculated on the basis of geometrical considerations and assuming the ideal model of a hexagonal array of non-intersecting cylindrical pores and a wall density of 2.2 g cm^{-3}; t – wall thickness, calculated as $t = a_o - D_p$ (DFT).

Table 2
Pore structural characteristics obtained by analysis of toluene adsorption isotherms at 298 K, before and after water adsorption (a.w.a.), of Al-MCM-41 samples prepared at ambient temperature and pressure[a]

Sample	A_{ext} ($m^2 g^{-1}$)	V_p ($cm^3 g^{-1}$)	$V_{0.9}$ ($cm^3 g^{-1}$)	D_p (nm)
Al-MCM-41(100)	36	0.76	0.80	3.85
a.w.a.	38	0.67	0.71	3.65
Al-MCM-41(50)	39	0.73	0.78	3.80
a.w.a.	38	0.65	0.69	3.65
Al-MCM-41(30)	34	0.66	0.70	3.75
a.w.a.	38	0.60	0.64	3.60
Al-MCM-41(15)	36	0.61	0.64	3.60
a.w.a.	38	0.53	0.57	3.40

[a] A_{ext} and V_p – external surface area and mesopore volume (in terms of equivalent liquid volume) obtained by the α_s method; $V_{0.9}$ – volume adsorbed at 0.9p° (in terms of equivalent liquid volume); D_p – mesopore diameter calculated using hybrid MC-DBdB method [40].

cycle that does not close at low pressures, the effect being more significant for the first water isotherm. The irreversibility of the isotherms at low pressure, which was also found with pure silica materials [24,57], is a reflection of the different type of interaction between water molecules and the adsorbent surface during the adsorption and desorption runs. Water adsorption on silica based materials involves, in addition to the physical adsorption, surface hydroxylation turning the surface more hydrophilic. During desorption at room temperature, only water physically adsorbed is removed from the surface.

With regard to the first water isotherm, it can be seen that samples with higher aluminium content adsorb a higher amount of water at low P/P_o, prior to pore filling, reflecting differences in the surface chemistry among samples. As expected, the surface of the samples with lower Si/Al is more hydrophilic in agreement with findings of others [58], and it is consistent with the previously observed increase in the acidic catalytic performance with the increase in aluminium content [37].

The gradual but clear shift of the condensation step towards lower P/P_o with the increase of the Al content is consistent with the decrease of the pore size in the same direction, as indicated by the nitrogen and toluene adsorption results. However, the big differences in the pressure at which the capillary condensation starts should also be related with the differences in the surface chemistry, namely the increase in the number of active sites with the increase in aluminium content, leading to an increase of the hydrophilic character. In fact, it was seen before that a shift in the condensation step in the opposite direction, to higher P/P_o, occurred when the MCM-41 surface was turned more hydrophobic by pyrolytic carbon deposition [31].

At the end of the desorption, and even after reoutgassing at 453 K, a small residual uptake of water was retained in the samples confirming that hydroxylation had occurred. Those residual uptakes were taken into account in the second isotherm for each sample, so that the amount adsorbed

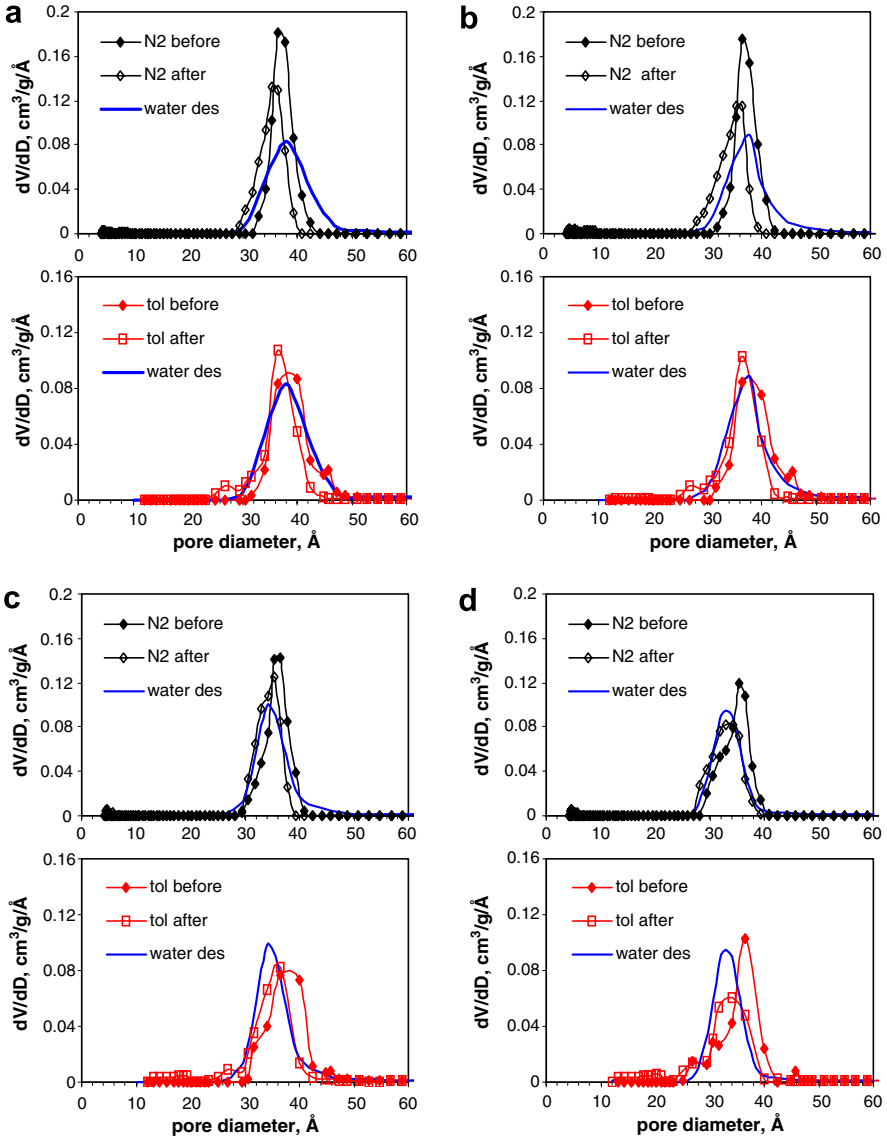

Fig. 4. Pore volume distributions prior to and after water adsorption (a.w.a) calculated from nitrogen isotherms, using NLDFT method [39] and from toluene isotherms using hybrid MC-DBdB method [40], of Al-MCM-41 materials with Si/Al of: (a) 100; (b) 50; (c) 30 and (d) 15. Also shown are pore volume distributions calculated from water desorption isotherms using DBdB method (see text).

on the second isotherm corresponds to the total amount adsorbed, i.e., the amount adsorbed during the second isotherm determination plus the amount of water that remained on the sample after outgassing.

The second water isotherm, obtained after outgassing of the sample is, in all cases, similar to the first one, continuing to exhibit a sharp pore filling step and the same hysteretic behaviour, despite the hysteresis loop now being much narrower. All samples adsorb a higher amount of water at low pressure during the second isotherm determination. The higher amount adsorbed arises from a stronger interaction between the water molecules and the surface, which was hydroxylated during the first exposure to water. The proximity between the initial part of the second adsorption branch and the first desorption branch indicates that during the first isotherm the hydroxylation of the surface was essentially complete. It is evident from Fig. 5 that the condensation inside the pores starts at much lower pressure than in the first isotherm, which can be associated with an increase in the strength of the adsorbate–adsorbent interaction. However, it can also result from a narrowing of the pores that occurred in all samples upon the first adsorption–desorption cycle and that will be confirmed in the following section.

For the purpose of comparison, the equivalent monolayer capacities were estimated assuming applicability of the BET equation to water adsorption. For the first adsorption run, the values vary from 1.4 H_2O/nm^2 for Al-MCM-41(100) to 3.2 H_2O/nm^2 for Al-MCM-41(15). Water adsorption increases after rehydroxylation of the surface, i.e., 3.6 H_2O/nm^2 for Al-MCM-41(100), and 5.6 H_2O/nm^2 for Al-MCM-41(15). Although values for non-

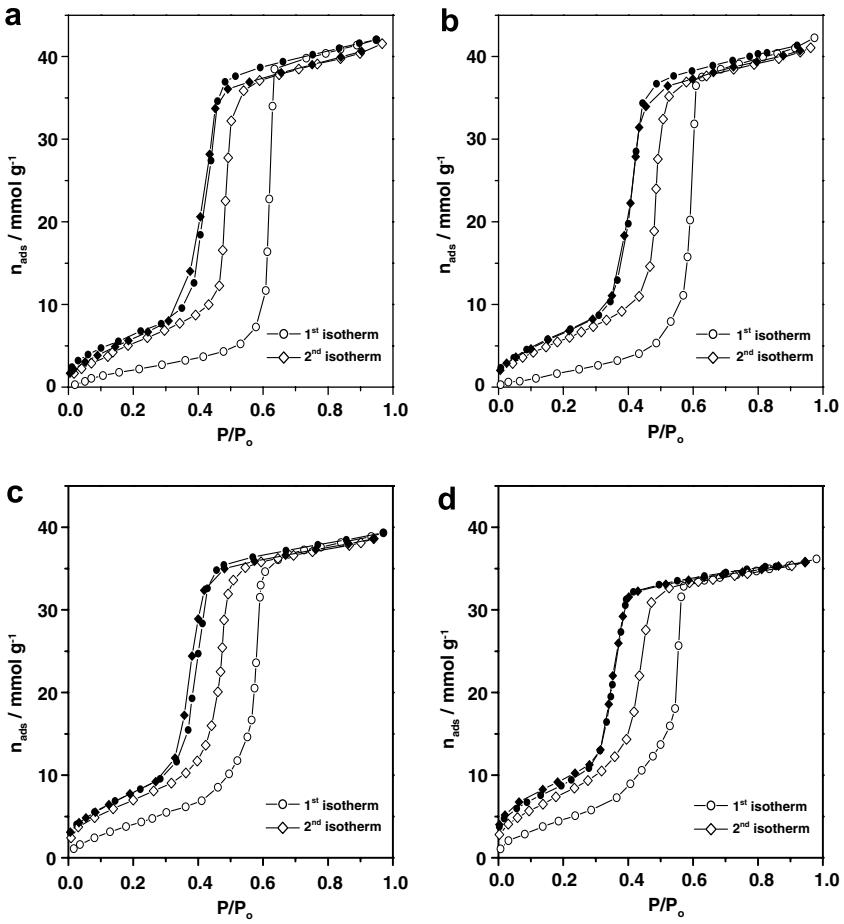

Fig. 5. Two consecutive water adsorption isotherms at 298 K on Al-MCM-41 materials with Si/Al of: (a) 100; (b) 50; (c) 30 and (d) 15 (empty symbols: adsorption, filled symbols: desorption).

porous silicas or aluminas vary depending on the type and pretreatment [59,60], our values are in between some reported for non-porous silica (e.g. 0.4 and 1.4 H_2O/nm^2 respectively for dehydroxylated silica and partially hydroxylated silica TK800 [59]) and alumina (e.g. 7.8 H_2O/nm^2 as calculated from data of Naono [47]). This is not surprising as we have previously shown [37] that the samples contain mainly framework aluminium (tetrahedrally coordinated) which alters the surface chemical properties, in comparison with pure silica, resulting in acidic properties which increase with increasing Al content, and the extraframework aluminium (octahedrally coordinated in alumina) exist in a lower proportion. In addition, we should stress that the values presented merely allow an appreciation in relative terms of the effect of Al content on these samples which were prepared in the same conditions and the differences between the first and second runs. The adsorbed values in this low pressure region are very sensitive to the surface chemistry and, as was pointed out [6], surface chemical properties depend on the sample preparation, including synthesis and calcination conditions. This would obviously reflect on the specific adsorption of water in the low pressure region and therefore it is expected that the absolute values obtained will differ between aluminosilicate samples prepared by different methods.

Besides the changes in the surface chemistry, the water adsorption results also give indication about eventual structural alterations resulting from exposure to water vapour. Considering the total water uptakes obtained at 0.9P$_o$, presented in Table 3, it can be noticed that the values for the second runs are identical or only slightly lower than those corresponding to the first isotherm, which is in marked contrast with the behaviour of pure silica MCM-41 for which the limiting uptakes on repeat runs were significantly reduced. The similarity of the $V_{0.9}$ values in the

Table 3
Results of the analysis of water vapour isotherms at 298 K obtained on Al-MCM-41 samples prepared at ambient temperature and pressure[a]

Sample	$V_{0.9}(1)$ (cm^3 g^{-1})	$V_{0.9}(2)$ (cm^3 g^{-1})	D_p (nm)
Al-MCM-41(100)	0.75	0.73	3.80
Al-MCM-41(50)	0.74	0.73	3.70
Al-MCM-41(30)	0.70	0.69	3.45
Al-MCM-41(15)	0.64	0.64	3.30

[a] $V_{0.9}(1)$, $V_{0.9}(2)$ – volume adsorbed at 0.9p° (in terms of equivalent liquid volume) on first and second adsorption isotherms; D_p – mesopore diameter calculated using DBdB method (see text).

two consecutive runs, indicates that no significant alterations occurred between the first measurement and the second and, in addition, that if any structural changes occurred they were mainly during the first adsorption but not during the desorption. This is also in contrast with what was found with pure silica grades, which indicated that structural changes occurred also during desorption of water [24]. Despite the differences between $V_{0.9}$ of the two runs being null or very small, a tendency of increasing difference with decreasing metal content is observed, suggesting that samples Al-MCM-41(100) and Al-MCM-41(50) are slightly less stable towards water vapour than Al-MCM-41(30) and Al-MCM-41(15).

To assess the changes in the pore structure of the samples due to water adsorption, we have also calculated the pore size distributions from water desorption branches (Fig. 4) using the DBdB approximation described above. Several features are worth mentioning. First, the pore sizes determined from water desorption isotherms are in good agreement with nitrogen and toluene measurements. For samples with low Al content, e.g. Al-MCM-41(100) and Al-MCM-41(50), the pore size obtained from water is in a somewhat better agreement with nitrogen and toluene pore sizes determined before water adsorption, while for samples with high Al content (Al-MCM-41(30) and Al-MCM-41(15)), water pore size is in a better agreement with the pore size obtained after sample exposure to water. It is also remarkable that for samples exposed to water, the widths of nitrogen, toluene and water pore size distributions are in excellent agreement with each other. This means that the water desorption isotherm can be considered as an equilibrium branch, suitable for pore size distribution calculations in materials with uniform cylindrical pores. It should be noted however, that the agreement in the absolute values of pore diameters calculated from the macroscopic DBdB theory, and those calculated from more advanced NLDFT and MC methods, is due to our choice of the disjoining pressure isotherm on pure alumina surface, which exhibits 1.4–2.2 times higher monolayer adsorption per unit area than was estimated for our samples. Had we used the isotherm on a silica surface, the pore diameters calculated from DBdB would have been underestimated, as was observed for nitrogen and argon adsorption [43]. The second feature is that we did not find any noticeable difference between the pore size distributions calculated from the first and second water desorption isotherms. This also indicates that the pore structure of the samples does not change between the first and second water isotherm measurements although the surface chemistry changes dramatically as is evident from the adsorption branches.

A global analysis of the results so far presented allows us to conclude that, taking into account the prolonged contact with pure water vapour and that samples were submitted to two cycles of water adsorption–desorption and also desorption at 453 K, the Al-MCM-41 with Si/Al between 100 and 15 prepared by this room temperature procedure are quite stable in the presence of water vapour at 298 K, the samples with higher Al content being slightly more stable.

3.3. Characterisation of the samples exposed to water by XRD, nitrogen and toluene adsorption

The results presented in Figs. 1–3 and Tables 1 and 2, clearly indicate that the materials still retain considerable structural ordering and high pore volumes and that structural alterations occurred to a much lesser extent than with the corresponding pure silica materials prepared by a similar method and also with an hydrothermally synthesised material [24].

In all cases, there is a decrease in the total surface area and pore volume, although not very accentuated (between 3–7% in surface area and 8–16% in nitrogen pore volume). In addition, it is evident that there is a reduction in pore size and a loss of uniformity of the pore structure is also observed, as the capillary condensation steps on the toluene and nitrogen isotherms are less vertical than prior to water adsorption, this being particularly obvious in the toluene isotherms. These features are confirmed by the pore size distributions.

Nevertheless, the overall shape of the isotherms is identical to those obtained prior to water adsorption, indicating that the structure was not significantly altered even after the second exposure to water and the desorption cycle. The X-ray diffraction data confirms this conclusion. In all cases, the pattern continues to exhibit three relatively well defined peaks. However, a slight loss of structural regularity occurs since, in all cases, the intensity of the peaks diminishes and the fourth peak present on the initial patterns of Al-MCM-41(100) and Al-MCM-41(50) has completely disappeared.

Furthermore, it can seen that, with the exception of Al-MCM-41(100), the values of a_o remain practically constant, which indicates that the reduction in pore size that occurred is basically a consequence of the hydroxylation during the first isotherm leading to an increase in wall thickness as shown in Table 1 and not a result of a partial collapse of the pore structure.

Pore narrowing can account partially for the decrease in nitrogen and toluene pore volumes. If we assume a model of cylindrical pores, the ratio of pore volume before and after water exposure should be equal to the ratio of the square of the pore radius. This is the case for Al-MCM-41(15) when considering the nitrogen results, suggesting that pore narrowing can be the sole factor leading to the decrease of pore volume for this sample. It should be noted that pore narrowing should also lead to a decrease in the uptake of water adsorption for the second run at high relative pressures higher than that appearing in Fig. 5 and Table 3. However it should be remembered that the amount adsorbed on the second isotherm corresponds to the total amount adsorbed, including that remaining after the first isotherm. If we consider only the amount adsorbed

during the second isotherm, neglecting that retained after outgassing then, in all cases, the water uptakes at high relative pressures are slightly below those on the first one which is then consistent with the decrease in the pore size of the MCM-41 materials.

If the same comparison is done as previously of hydraulic pore widths (not shown) using the results from α_s analysis, and the NLDFT pore sizes, values for the nitrogen cross sectional area between 0.131 nm^2 and 0.134 nm^2, lower than on the original samples, are obtained. Changes of cross sectional area with the degree of hydroxylation have also been observed for a number of oxides [49,61].

An interesting feature regarding the toluene adsorption is that for all samples the amount adsorbed before capillary condensation is superior to that adsorbed by the original sample. The results suggest that the toluene molecule is sensitive to the surface chemistry and it interacts specifically. In this way, a stronger interaction occurs with the surface richer in hydroxyl groups. In fact, adsorption of toluene on non-porous silicas indicates a certain degree of specificity associated with adsorbate–adsorbent interaction [62]. Somewhat stronger interaction of toluene with the pore surfaces after exposure to water vapour is indirectly evidenced from the broadening of the pore size distributions. It should be noted that the model for calculating pore size distributions from toluene isotherms had been developed for pure silica MCM-41 materials. Application of this model to materials with higher number of hydroxyl groups and/or with high aluminium content may result in a broadening of the pore size distributions and appearance of small amounts of artificial pores at the lower end of the PSD, e.g. below 3 nm (Fig. 4).

Analysing in more detail the nitrogen and toluene data obtained prior to and after water adsorption we can get some information about the textural changes that occurred. If we calculate the ratio between $V_{0.9}$ after water adsorption and before for toluene and nitrogen we see that for the hydrocarbon, the values obtained are 0.89 or very close in all cases, whereas those corresponding to nitrogen increase steadily from 0.84 for Al-MCM-41(100) to 0.94 for Al-MCM-41(15). The results indicate that the interaction of water with the surface affects differently the adsorption of toluene and nitrogen, having a more negative effect on the nitrogen adsorption for the samples with the lowest Al content and, on the contrary, a more negative effect on the toluene adsorption for the Al-MCM-41(30) and Al-MCM-41(15).

Considering first the samples with Si/Al of 30 and 15, the results can have an easy explanation: the hydroxylation of the surface and consequent pore narrowing changed the space inside the channels and the bulkier toluene molecules are not capable of a space occupation as efficient as the smaller nitrogen molecules and so the toluene total uptake experiences a higher decrease.

With regard to the samples Al-MCM-41(100) and Al-MCM-41(50) the opposite situation is observed. Since it does not seem probable that after water adsorption the bulky toluene molecules can fit in spaces where nitrogen did not have access, a possible explanation is that there were spaces that became unavailable for nitrogen which were already (before water adsorption) not accessible to the toluene molecules. This could be related with defects on the pore wall surfaces where nitrogen can fit but toluene can not. During water adsorption these defects are blocked, becoming inaccessible to nitrogen and so a higher decrease in the pore volume is observed for this adsorptive. The fact that similar results are not observed with samples Al-MCM-41(30) and Al-MCM-41(15) suggests a lower degree of these defects.

3.4. Stability of the Al-MCM-41 samples

Comparing the results obtained here with those presented previously for the adsorption of water on pure silica MCM-41 materials synthesised at room temperature [24] it is clear that a different behaviour towards water vapour is exhibited by the Al-MCM-41 materials, even by those with the lowest Al content.

Although a decrease in the pore size and capacity is observed for all the Al-MCM-41 samples after exposure to water vapour, it is not comparable with the changes that occur with the Si-MCM-41 materials. These results clearly show that the introduction of aluminium stabilises the structure with respect to prolonged exposure to pure water vapour at 298 K and that the degree of stabilisation depends on the amount of aluminium present. It is interesting to note that addition of aluminium, either by grafting or by direct synthesis, was also found to significantly increase the aqueous stability of mesoporous silica thin films [63].

Several explanations can be put forward to explain the improvement of the stability of the Al-MCM-41 samples towards water vapour at 298 K.

A possible explanation is related with the extraframework, octahedrally coordinated aluminium. ^{27}Al MAS NMR spectra have shown that some dealumination occurs upon calcination with formation of a small proportion of hexacoordinated aluminium [37]. Indeed, some studies on the hydrothermal stability of aluminosilicates, including Al-MCM-41 [17] and zeolite materials [64] indicate that extraframework Al increases this type of stability by acting as a protective barrier over the surface. This protective layer hides the surface silanol groups making their reaction with the water molecules impossible. The presence of aluminium not incorporated in the walls, even in a small proportion, can explain the stability of the samples Al-MCM-41(30) and Al-MCM-41(15), by avoiding the reaction of the silanol groups with water. These extraframework species could be a major factor accounting for the roughness of the pore wall surfaces for these higher content samples. However, it does not seem reasonable that the extraframework aluminium could be capable of covering almost all the very high surface area, especially in the case of samples with lower Al content (Si/Al of

100 and 50), that although less stable than those with Si/Al of 30 and 15, are still much more stable than the pure silica material. Therefore, the extraframework Al can play a role in the stabilisation of the Al-MCM-41 structure but it can not be the only factor. In fact, Mokaya [14] tested the hydrothermal stability of an Al-MCM-41 material presenting only extraframework aluminium and found that this sample was not as stable as those with aluminium also incorporated on the walls.

Consequently, it seems likely that the tetracoordinated aluminium, incorporated in the walls, has also a stabilisation effect. One of the reasons could be the improvement of the polymerisation degree of the walls, namely at the pore surfaces, due to the formation of stronger Si–O–Al bonds, leading to denser walls and less surface defects. This hypothesis would be in agreement with the nitrogen and toluene adsorption results presented before. The comparison of the results before and after water adsorption for the two adsorptives made in the previous section could be explained by the presence of defects on the pore wall surfaces of samples Al-MCM-41(100) and Al-MCM-41(50). Those defects, that could be the major factor accounting for the surface roughness in these lower Al content samples, would be related with a low degree of polymerisation of the surface of the walls and therefore they would be areas highly susceptible to the attack of water molecules. Upon hydroxylation these defects would be blocked to nitrogen molecules. Therefore, the results indicate that this type of defects decreases with the increase of the aluminium content as the ratio of the $V_{0.9}$ after and prior to water adsorption for nitrogen of sample Al-MCM-41(50) is higher than that of Si/Al = 100. So, we can conclude that the aluminium decreases the presence of these defects which leads to an increase in the stability.

Another plausible factor that may account for the good Al-MCM-41 stability is related with its acidity. Taking into account that these Al-MCM-41 present Brønsted acid sites, as previously shown by the catalytic results [37], and that during the water vapour adsorption capillary condensation takes place inside the pores, it is possible that proton donation from the adsorbent to water occurs, turning the environment inside the pores slightly acidic. It is known that the water attack on Si–O–Si bonds and terminal OH groups is catalysed by OH^-, which is the reason why desilication of zeolites is accomplished in alkaline solutions [65]. In opposition, Al–O–Si bond dissociation is catalysed by acids and so aluminosilicates are dealuminated by acid solutions especially at high temperatures. In fact, other authors [66] have found that the structure of pure silica and aluminium containing MCM-41 was completely destroyed in basic solutions, due to rapid hydrolysis of Si–O–Si bonds, while the changes were much less in water and acidic solution as the hydrolysis of siloxane bonds was slower. No dealumination was found in water but it occurred in acidic solution leading to bigger changes. However, the decrease in surface area was more pronounced than in our work as the solution was strongly acid (pH 2).

So, it is possible that the mild acidity of Al-MCM-41, associated with tetracoordinated aluminium which was previously found to be the predominant species in the room temperature synthesised samples, turns the attack on siloxane linkages by water more difficult, and consequently less siloxane bond dissociation occurs. In addition, it is not sufficient, as well as the temperature is not high enough, to cause dealumination which would lead to more pronounced structural alterations than those observed. Therefore, the increase of the acid sites can be an additional factor contributing to the increase of the structural stability of Al-MCM-41 as the Al content increases.

4. Conclusions

The results provide evidence that the introduction of Al in the silica matrix, by this room temperature synthesis method, using tetraethoxysilane and aluminium sulfate, promotes a considerable improvement of the stability towards water vapour at 298 K. Moreover, the stability depends on the aluminium content as the greater improvement was found for samples having the lowest Si/Al ratios (15 and 30), in spite of the slight increase in the hydrophilicity of the surface.

The detailed analysis of the different approaches considered, allowed us to obtain a consistent picture of the effects of interaction with water vapour and to put forward explanations for the enhancement in stability due to aluminium.

After the prolonged exposure to water vapour during the determination of two consecutive water adsorption–desorption isotherms, only a slight loss of long range structural order has occurred and this was accompanied by a small decrease in pore volume (8–16%), total surface area (3–7%), pore size (3–5%) and pore size uniformity, but with practically no alteration in the external surface area. The changes that occurred can be attributed essentially to the hydroxylation of the surface during water isotherms determination and mainly during the first adsorption run, in particular for the samples with higher Al content.

The high stability of the materials can result from extraframework aluminium as well as aluminium incorporated in the pore walls. On the one hand, hexacoordinated aluminium species extra-walls, even in small proportion, could act as a protective barrier, not allowing the reaction of water molecules with Si–O–Si bonds to occur. On the other hand, the incorporation of tetracoordinated aluminium could promote a higher degree of polymerisation of the pore wall surfaces. In addition, the mild acidity of Al-MCM-41 materials could make the attack of water on siloxane linkages more difficult, thereby avoiding their dissociation.

Acknowledgments

This work was financially supported by the Fundação para a Ciência e a Tecnologia (FCT, Portugal) and the Fundo Europeu para o Desenvolvimento Regional (FED-

ER) (Project No. POCTI/CTM/45859/2002). P.A.R. thanks FCT for PhD Grant No. SFRH\BD\17713\2004.

References

[1] C.T. Kresge, M.E. Leonowicz, W.J. Roth, J.C. Vartuli, J.S. Beck, Nature 359 (1992) 710.
[2] J.S. Beck, J.C. Vartuli, W.J. Roth, M.E. Leonowicz, C.T. Kresge, K.D. Schmidt, C.T-W. Chu, D.H. Olson, E.W. Sheppard, S.B. McCullen, J.B. Higgins, J.C. Schlenker, J. Am. Chem. Soc. 114 (1992) 10834.
[3] A. Corma, M.S. Grande, V. Gonzalez-Alfaro, A.V. Orchilles, J. Catal. 159 (1996) 375.
[4] A. Corma, Chem. Rev. 97 (1997) 2373.
[5] G. Øye, J. Sjöblom, M. Stöcker, Adv. Colloid Interf. Sci. 89–90 (2001) 439.
[6] D. Brunel, A.C. Blanc, A. Galarneau, F. Fajula, Catal. Today 73 (2002) 139.
[7] A. Tagushi, F. Schüth, Micropor. Mesopor. Mater. 77 (2005) 1.
[8] G. Øye, W.R. Glomm, T. Vrålstad, S. Volden, H. Magnusson, M. Stöcker, J. Sjöblom, Adv. Colloid Interf. Sci. 123–126 (2006) 17.
[9] T.R. Pauly, V. Petkov, Y. Liu, S.J.L. Billinge, T.J. Pinnavaia, J. Am. Chem. Soc. 124 (2002) 97.
[10] A. Davidson, Curr. Opin. Colloid Interf. Sci. 7 (2002) 92.
[11] T. Linssen, K. Cassiers, P. Cool, E.F. Vansant, Adv. Colloid Interf. Sci. 103 (2003) 121.
[12] J.M. Kim, J.H. Kwak, S. Jun, R. Ryoo, J. Phys. Chem. 99 (1995) 16742.
[13] S.C. Shen, S. Kawi, J. Phys. Chem. B 103 (1999) 8870.
[14] R. Mokaya, J. Phys. Chem. B 104 (2000) 8279.
[15] X.S. Zhao, G.-Q. Lu, X. Hu, Micropor. Mesopor. Mater. 41 (2000) 37.
[16] R. Mokaya, W. Jones, Chem. Commun. (1998) 1839.
[17] R. Mokaya, Chem. Commun. (2001) 633.
[18] S.C. Shen, S. Kawi, Langmuir 18 (2002) 4720.
[19] J.P. Lourenço, A. Fernandes, C. Henriques, M.F. Ribeiro, Micropor. Mesopor. Mater. 94 (2006) 56.
[20] N. Coustel, F. Di Renzo, F. Fajula, J. Chem. Soc., Chem. Commun. (1994) 967.
[21] R. Mokaya, J. Phys. Chem. B 103 (1999) 10204.
[22] K.A. Koyano, T. Tatsumi, Y. Tanaka, S. Nakata, J. Phys. Chem. B 101 (1997) 9436.
[23] X.S. Zhao, F. Audsley, G.-Q. Lu, J. Phys. Chem. B 102 (1998) 4143.
[24] M.M.L. Ribeiro Carrott, A.J.E. Candeias, P.J.M. Carrott, K.K. Unger, Langmuir 15 (1999) 8895.
[25] N. Igarashi, K.A. Koyano, Y. Tanaka, S. Nakata, K. Hashimoto, T. Tatsumi, Micropor. Mesopor. Mater. 59 (2003) 43.
[26] X.S. Zhao, G.-Q. Lu, J. Phys. Chem. B 102 (1998) 1556.
[27] C.P. Jaroniec, M. Kruk, M. Jaroniec, A. Sayari, J. Phys. Chem. B 102 (1998) 5503.
[28] V. Antochshuk, M. Jaroniec, Chem. Commun. (1999) 2373.
[29] A. Matsumoto, H. Misran, K. Tsutsumi, Langmuir 20 (2004) 7139.
[30] J.M. Kisler, M.L. Gee, G.W. Stevens, A.J. O'Connor, Chem. Mater. 15 (2003) 619.
[31] M.M.L. Ribeiro Carrott, A.J.E. Candeias, P.J.M. Carrott, K.S.W. Sing, K.K. Unger, Langmuir 16 (2000) 9103.
[32] A.E. Candeias, M.M.L. Ribeiro Carrott, P.J.M. Carrott, K. Schumacher, M. Grun, K.K. Unger, in: F. Rodriguez-Reinoso, B. McEnaney, J. Rouquerol, K.K. Unger (Eds.), Characterisation of Porous Solids VI, Studies in Surface Science and Catalysis, vol. 144, Elsevier, Amsterdam, 2002, p. 363.
[33] P.J. Branton, P.G. Hall, K.S.W. Sing, Adsorption 1 (1995) 77.
[34] P.L. Llewellyn, F. Schüth, Y. Grillet, F. Rouquerol, J. Rouquerol, K.K. Unger, Langmuir 11 (1995) 574.
[35] A. Matsumoto, H. Chen, K. Tutsumi, M. Grün, K. Unger, Micropor. Mesopor. Mater. 32 (1999) 55.
[36] M.M.L. Ribeiro Carrott, C. Galacho, F.L. Conceição, P.J.M. Carrott, in: P.L. Llewellyn, J. Rouquerol, F. Rodriguez-Reinoso, N. Seaton (Eds.), Characterisation of Porous Solids VII, Studies in Surface Science and Catalysis, vol. 160, Elsevier, Amsterdam, 2006, p. 567.
[37] M.M.L. Ribeiro Carrott, F.L. Conceição, J.M. Lopes, P.J.M. Carrott, C. Bernardes, J. Rocha, F. Ramôa Ribeiro, Micropor. Mesopor. Mater. 92 (2006) 270.
[38] R.C. Reid, J.M. Prausnitz, B.E. Poling, The Properties of Gases and Liquids, McGraw-Hill, New York, 1986.
[39] P.I. Ravikovitch, A.V. Neimark, Colloid Surf. A 187–188 (2001) 11.
[40] P.I. Ravikovitch, A. Vishnyakov, A.V. Neimark, M.M.L. Ribeiro Carrott, P.A. Russo, P.J.M. Carrott, Langmuir 22 (2006) 513.
[41] B.V. Derjaguin, Acta Phys. Chim. 12 (1940) 181.
[42] J.C. Broekhof, J.H. de Boer, J. Catal. 10 (1968) 368.
[43] A.V. Neimark, P.I. Ravikovitch, Micropor. Mesopor. Mater. 44 (2001) 697.
[44] S.J. Gregg, K.S.W. Sing, Adsorption Surface Area and Porosity, 2nd ed., Academic Press, London, 1982.
[45] J. Hagymassy Jr., S. Brunauer, R.Sh. Mikhail, J. Colloid Interf. Sci. 29 (1969) 485.
[46] A. Raoof, J-P. Guilbaud, H. Van Damme, P. Porion, P. Levitz, J. Colloid Interf. Sci. 206 (1998) 1.
[47] H. Naono, M. Hakuman, J. Colliod Interf. Sci. 158 (1993) 19.
[48] C. Galacho, M.M.L. Ribeiro Carrott, P.J.M. Carrott, Micropor. Mesopor. Mater., doi: 10.1016/j.micromeso.2006.11.018.
[49] F. Rouquerol, J. Rouquerol, K.S.W. Sing, Adsorption by Powders and Porous Solids, Academic Press, London, 1999.
[50] M.M.L. Ribeiro Carrott, A.J. Candeias, P.J.M. Carrott, P.I. Ravikovitch, A.V. Neimark, A.D. Sequeira, Micropor. Mesopor. Mater. 47 (2001) 323.
[51] V.B. Fenelonov, A.Yu. Derevyankin, S.D. Kirik, L.A. Solovyov, A.N. Shmakov, J.-L. Bonardet, A. Gedeon, V.N. Romannikov, Micropor. Mesopor. Mater. 44–45 (2001) 33.
[52] N. Muroyama, T. Ohsuna, R. Ryoo, Y. Kubota, O. Terasaki, J. Phys. Chem. B 110 (2006) 10630.
[53] P.I. Ravikovitch, A.V. Neimark, Langmuir 22 (2006) 11171.
[54] A. Galarneau, D. Desplantier, R. Dutartre, F. Di Renzo, Micropor. Mesopor. Mater. 27 (1999) 297.
[55] P.L. Llewellyn, C. Sauerland, C. Martin, Y. Grillet, J.-P. Coulomb, F. Rouquerol, J. Rouquerol, in: B. McEnaney, T.J. Mays, J. Rouquerol, F. Rodriguez-Reinoso, K.S.W. Sing, K.K. Unger (Eds.), Characterisation of Porous Solids IV, Royal Society of Chemistry, London, 1997, p. 111.
[56] M. Kruk, M. Jaroniec, Langmuir 15 (1999) 5683.
[57] H. Naono, M. Hakuman, T. Tanaka, N. Tamura, K. Nakai, J. Colloid Interf. Sci. 225 (2000) 411.
[58] M. Rozwadowski, M. Lezanska, J. Wloch, K. Erdmann, R. Golembiewski, J. Kornatowski, Langmuir 17 (2001) 2112.
[59] F.S. Baker, K.S.W. Sing, J. Colloid Interf. Sci. 55 (1976) 605.
[60] J.D. Carruthers, D.A. Payne, K.S.W. Sing, L.J. Stryker, J. Colloid Interf. Sci. 36 (1971) 205.
[61] J. Rouquerol, F. Rouquerol, C. Pérès, Y. Grillet, M. Boudellal, in: S.J. Gregg, K.S.W. Sing, H.F. Stoeckli (Eds.), Characterisation of Porous Solids, Society of Chemical Industry, London, 1979, p. 107.
[62] L.J.M. Schlangen, L.K. Koopal, M.A.C. Stuart, J. Lyklema, M. Robin, H. Toulhoat, Langmuir 11 (1995) 1701.
[63] D.R. Dunphy, S. Singer, A.W. Cook, B. Smarsly, D.A. Doshi, C.J. Brinker, Langmuir 19 (2003) 10403.
[64] W. Lutz, W. Gessner, R. Bertram, I. Pitsch, R. Fricke, Micropor. Mater. 12 (1997) 131.
[65] H.K. Beyer, in: H.G. Karge, J. Weitkamp (Eds.), Post-synthesis Modification I, Molecular Sieves – Science and Technology, vol. 3, Springer-Verlag, Heidelberg, 2002, p. 203.
[66] D. Trong On, S.M.J. Zaidi, S. Kaliaguine, Micropor. Mesopor. Mater. 22 (1998) 211.